Supporting Information

Photoinduced Defect Engineering: Enhanced Photocatalytic Performance of 3D BiOCl Nanoclusters with Abundant Oxygen Vacancies

Qi Shen,[a,#] Junnuan Wang,[a,#] Bo Xu,[a] Guangning Liu,[a] Guozhu Chen,[a] Huanyu Huo,[c] Yiqiang Sun,[a,b,c,#,*] Bingqiang Cao,[b,*] Cuncheng Li,[a,*]

---

a School of Chemistry and Chemical Engineering, University of Jinan, Jinan 250022, China

b School of Materials Science And Engineering, University of Jinan, Jinan 250022, China

c Foshan (Southern China) Institute for New Materials, Foshan 528200, Guangdong, China

EXPERIMENTAL SECTION

Materials

Ethylene glycol (EG, 99.9 %) and ethanol (99.9 %) were purchased from Xilong Chemical Industry Incorporated Co. Ltd. Polyvinyl pyrrolidone (PVP, Mw ≈ 40,000) were obtained from Sigma-Aldrich. Bismuth chloride ($BiCl_3$, 99 %), ciprofloxacin (CIP, 98 %), benzoquinone (BQ, 97 %), isopropyl alcohol (IPA, 98 %), and disodium ethylenediaminetetraac-etate (EDTA-2Na, 98 %) were purchased from Macklin. Deionized water was prepared with a Milli-Q water purification system. All chemicals were analytical grade and used without further purification.

Representative Synthesis of BiOCl-NCs

For a typical synthesis of BiOCl-NCs, 15 mL of 50 mM $BiCl_3$ glycol solution and 0.38 mL of 2 M PVP aqueous solution were successively injected into 9 mL EG solution in a 50 mL plastic centrifuge tube with vigorously magnetic stirring. Subsequently, 6 mL of deionized water was quickly added into the tube. After stirring for 10 minutes, a uniform, light milk-white colloid solution would be formed at the colorless transparent precursor solution. The final volume ratio of water to EG in the reaction mixture solution is 1:4 and the concentrations of PVP and $BiCl_3$ were 25 mM and 25 mM, respectively. Finally, the system was statically kept on room temperature for 12 h. The resulting precipitates were collected and washed with ethanol and deionized water thoroughly and dried at 100 ℃ in air. After the light irradiation for 10 min, the catalyst was collected and named BiOCl-NCs-OV.

Morphological Characterization

The products were characterized by transmission electron microscopy (TEM, JEM-1400), energy-dispersive X-ray spectroscopy (EDS), and high-resolution TEM (HRTEM, JEM-2100F). The samples for TEM examination were prepared by putting a droplet of the ethanol dispersed sample solution on a copper grids coated with thin carbon film and then drying at 60 °C in air. Powder X-ray diffraction (PXRD) patterns were recorded on a Rigaku Ultima IV X-ray diffractometer with Cu Kα radiation

(λ=0.15418 nm) by depositing the products on glass slides. Thermo ESCALAB 250 equipped with a monochromatic Al Kα X-ray source (1486.6 eV) was employed for the X-ray photoelectron spectroscopy (XPS) analysis. The binding energy of C1s at 284.8 eV was utilized as a reference to calibrate those of others elements. Nitrogen (N_2) adsorption-desorption isotherms were measured on a Micromeritics TriStar II 3020 instrument at 77 K. Before measurement, the samples were degassed and dried at 200 °C under vacuum for 4h. The specific surface area was calculated according to the Brunauer-Emmett-Teller (BET) analysis and the pore size distribution was determined by a desorption isotherm via using the Barrett-Joyner-Halenda (BJH) method. Fourier transform infrared spectroscopies (FTIR) were conducted on a PerkinElmer VERTEX 70 FTIR spectrophotometer. UV-Vis-NIR diffuse reflectance spectra (DRS) was performed on a Shimadzu UV-3101PC spectrophotometer in the wavelength range of 200 to 900 nm. A TG8121 Rigaku thermal analyzer was employed to record the thermogravimetric (TG) curve of the samples from 30 °C to 600 °C at a heating rate of 20 °C/min in the air atmosphere. Photoluminescence (PL) spectra and PL lifetime were recorded on Edinburgh FLS920 Multifunction Steady State and Transient State Fluorescence. Electron spin resonance (ESR) spectrum was obtained over an electron paramagnetic resonance spectrometer (JEX-X320, JEOL RESONANCE Inc.) at X-band at room temperature. The g-value was determined with the cwESR Simfonia Program from JEOL.

Photocatalytic Activity Measurements

The solar-motivated photocatalytic activities of BiOCl obtained at various conditions were assessed by the degradation of organic dye Rhodamine B (RhB) in an aqueous solution under a simulated sunlight irradiation. In a typical photodegradation test, 5 mg catalysts were firstly added to 99.8 mL deionized water to form a uniform suspension with a magnetic stirring. And then, 0.2 mL of 5 mM RhB aqueous solution was injected into the above suspension. The concentrations of RhB in the initial suspension is 0.01 mM. Before illumination, the above as-prepared mixture solutions were stirred for 20 min in dark environment till achieving an adsorption-desorption

equilibrium between pollutants and catalysts. A 300W Xenon lamp (Perfect Light PLS-SXE-300C) was served as a simulated sunlight source to conduct the photocatalytic test. The distance between the Xenon lamp and the suspension containing catalysts and RhB was about 25 cm. A circulating water system was employed to keep the reaction at 25 ^{o}C and to prevent thermal catalytic effect. The 2 mL suspension irradiated was sampled every 2 minutes during the photocatalytic experiments. The catalysts were removed from the harvested suspension by centrifugation. After centrifugation, the supernatant solution was collected and diluted 3 times for RhB with deionized water to measure the residue of RhB according to their future absorption in the UV-Vis spectra. The photocatalytic activity of BiOCl-NCs-OV in the cyclic experiments was also investigated through the following procedure: the suspensions containing BiOCl-NCs-OV and RhB were firstly stirred 20 min in darkness and then irradiated for 4 min using a 300 W Xenon lamp. Subsequently, 2 mL suspensions were extracted for measuring the degradation effect of RhB. While a given amount of RhB aqueous solution was added into the remaining suspensions again to respectively recover the RhB, concentration to 0.01 mM for the next degradation experiment.

The photocatalytic activities of BiOCl-NCs-OV were also evaluated by reduction of Cr(Ⅵ) under UV-visible light irradiation of a 300W Xe arc lamp. Potassium dichromate ($K_2Cr_2O_7$) was selected as a Cr(Ⅵ) compound. The photocatalytic reduction of Cr(Ⅵ) was performed at about 25 ℃ in a quartz reactor containing 20 mg photocatalyst and 40 ml of Cr(Ⅵ) solution (8 mg L^{-1} based on Cr in a dilute $K_2Cr_2O_7$ solution). The solution was stirred for 20 min in the dark to reach adsorption equilibrium and then was exposed to UV-visible light irradiation. The Cr content in the reaction solution was determined using the DPC method[1]. The photocatalytic efficiency was determined by dividing C/C_0, where C is the remained Cr(Ⅵ) concentration and C_0 is the initial Cr(Ⅵ) concentration.

Radical-trapping Experiments

Experiments were carried out to ascertain the active species participated in the degration reaction by employing carbon tetrachloride (CCl_4), isopropanol (IPA), disodium ethylenediaminetetraac-etate (EDTA-2Na), and benzoquinone (BQ) as electron (e^-) hydroxyl radical ($\cdot OH$), hole (h^+), and superoxide radical ($\cdot O_2^-$) scavengers, respectively. Similar to the photocatalytic activity measurement, a given amount of pollutants (RhB), BiOCl-NCs-OV, and scavengers (IPA, EDTA-2Na, or BQ) were sequentially added into 100 mL deionized water under stirring. And then, a 30 min dark adsorption process was performed prior to light illumination. After irradiation for a certain time, the suspensions were collected and the concentrations of the remnant pollutants were measured by the UV-Vis absorption. For comparison, the concentration of scavengers in all the radical-trapping experiments is 1 mM.

Photoelectrochemical measurement

Photo-electrochemical measurements were measured on a Solar-tron Analytical electrochemical analyzer (ModuLab XM) in a standard three electrode system by utilizing Pt foil as the counter electrode and Ag/AgCl (KCl, 3M) as a reference electrode. The indium doped tin oxide (ITO, China Guluo Glass Co., Ltd., Luoyang, China) substrates were cleaned sequentially by ultrasonication in distilled water, absolute ethanol, and isopropanol for 15 min. The working electrodes were prepared by spreading ethanol dispersed slurries of samples (10 mg in a 1 mL ethanol) onto the well-cleaned ITO glass substrates. Subsequently, the sample-coated substrates were dried in air for 10 min and the annealed at 100 ℃ for 30 min for electrochemical impedance spectroscopy (EIS) analysis, photocurrent response and Mott-Schottky plots (MS). In the photo-electrochemical measurements, all three electrodes were placed in a quartz cell containing 0.5 M Na_2SO_4 aqueous solution as the electrolyte which was bubbled by N_2 thoroughly to remove oxygen before the measurement. The transient photocurrent responses were conducted at a bias potential of 0.5 V under a 20 s on/off chopped illumination. The distance between the Xenon lamp and the working electrode was about 2 cm. EIS analysis was measured in the three-electrode system and recorded over a frequency range from 0.01 Hz to 1 MHz with current voltage amplitude of 0.01

V.

Density functional theory (DFT) calculations

We performed our calculations using the Vienna ab initio simulation package (VASP) with projector augmented wave (PAW) pseudopotentials and the generalized gradient approximation in the parameterization of Perdew, Burke, and Ernzerhof for the exchange-correlation functional. Bi 5d6s6p, O 2s2p, and Cl 2s2p electrons were treated as the valence electrons in the PAW potentials. A plane-wave energy cut-off of 500 eV was determined by the VASP PAW potential of O. All atoms were fully relaxed during structural relaxation until the atomic forces were smaller than 0.01 eV $Å^{-1}$. The lattice parameters of the optimized BiOCl are a=b=3.9057Å, and c=7.3388Å.

Figure S1. Schematic illustration of the synthesis procedure for the BiOCl-NCs-OV.

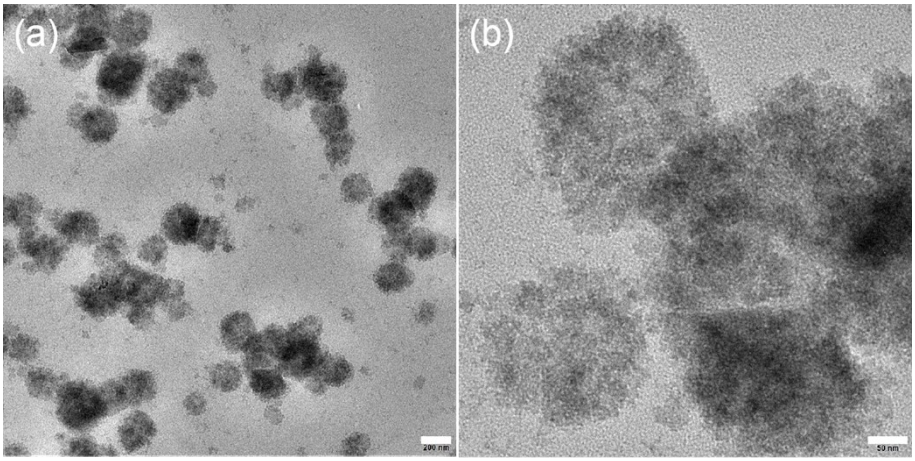

Figure S2. (a) Low-magnification and (b) high-magnification TEM images of BiOCl nanoclusters precursors.

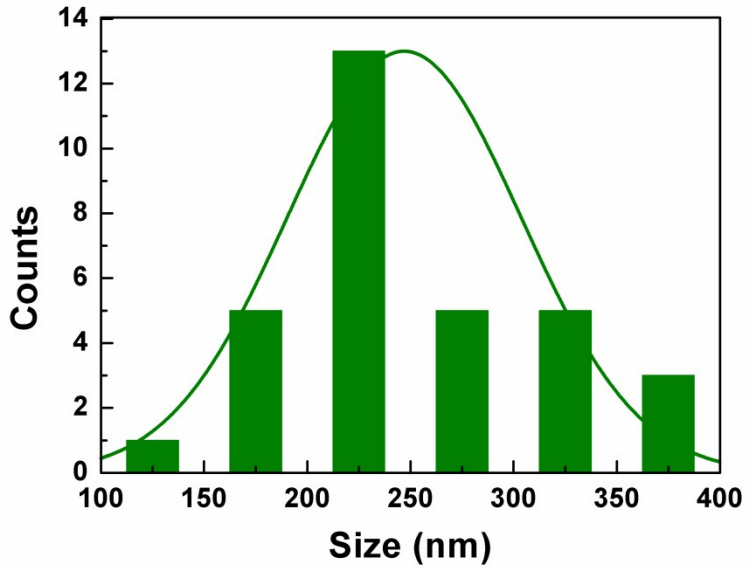

Figure S3. Size distribution of BiOCl nanoclusters precursors.

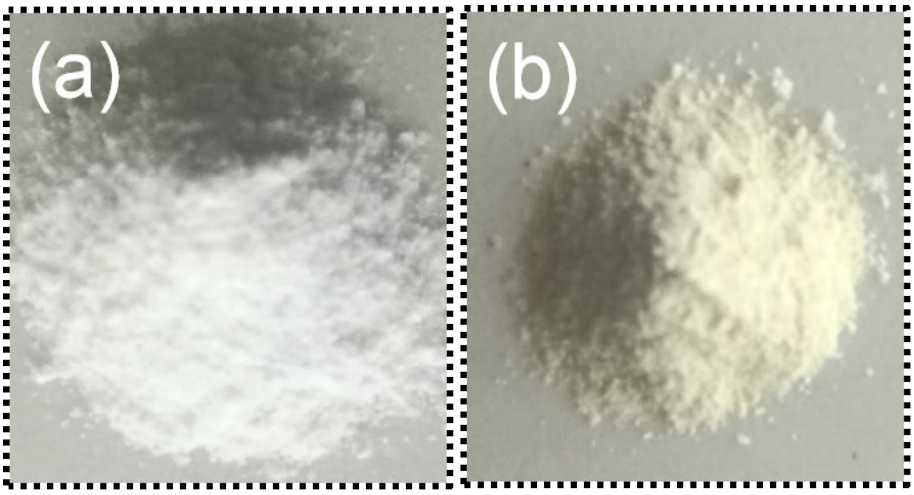

Figure S4. The photographic images of (a) BiOCl nanoclusters precursors and (b) BiOCl-NCs-OV.

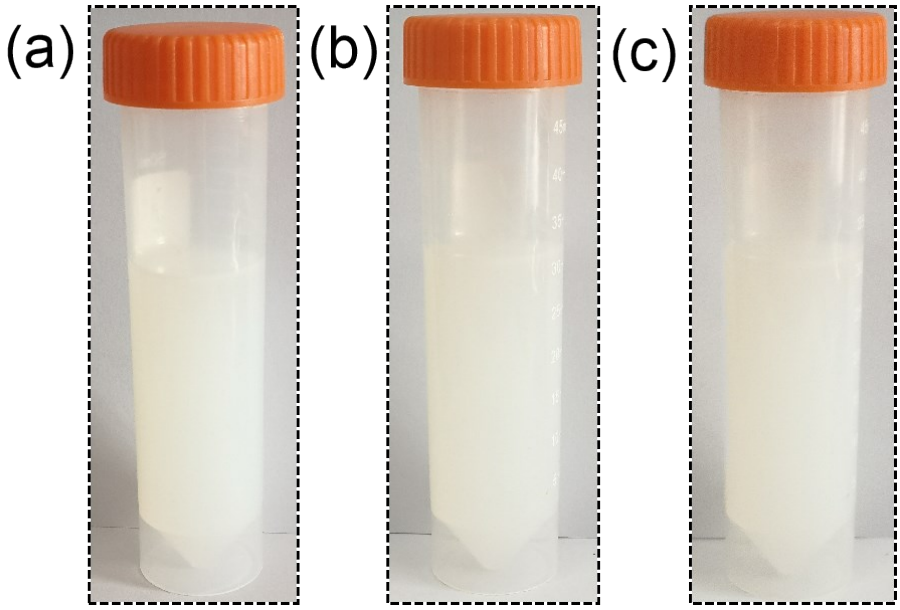

Figure S5. The photographic images of (a) BiOCl nanoclusters precursors and (b) BiOCl-NCs-OV.

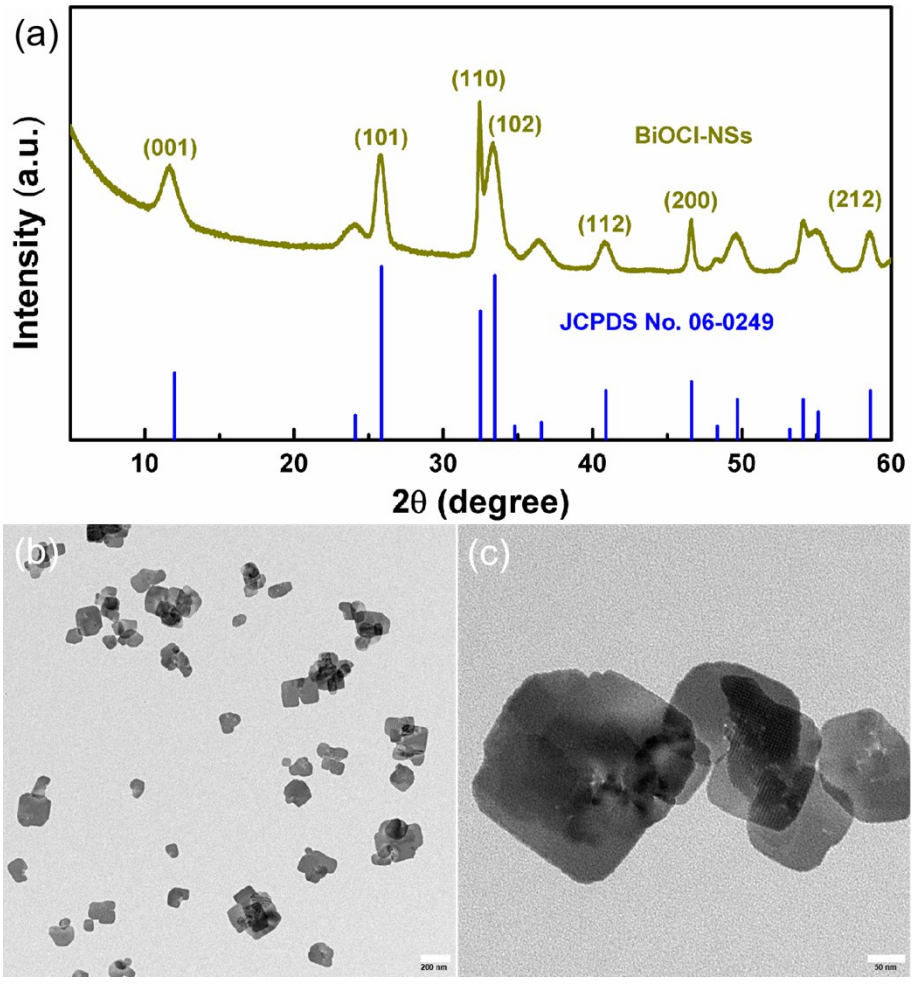

Figure S6. (a) XRD pattern, and (b, c) TEM images of traditional BiOCl-NSs.

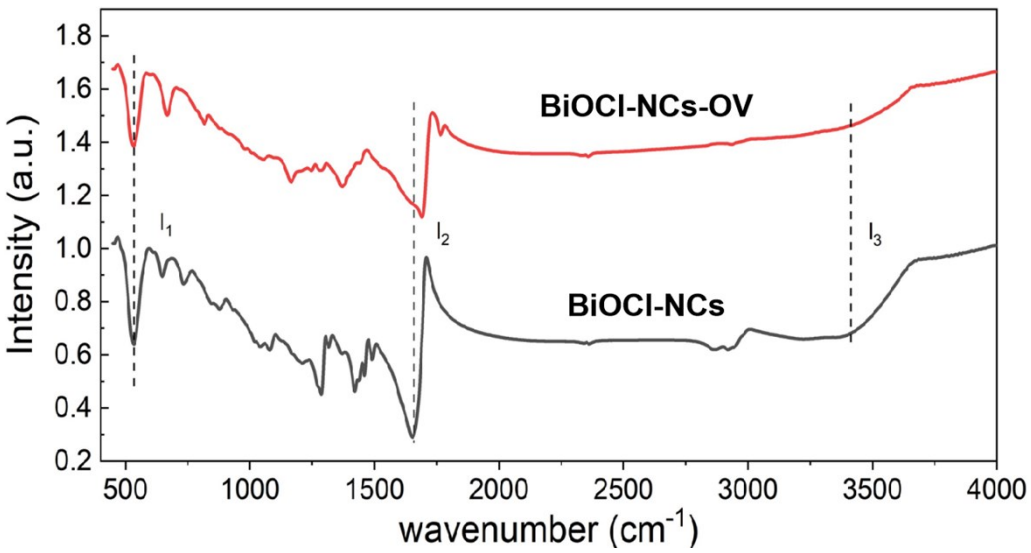

Figure S7. Normalized FT-IR spectra in the range 400-4000 cm^{-1}.

Sample	I1(563)	I2(1640)	I3(3400)	I3(3400)/I1(563)	I2(1640)/I1(563)
BiOCl-NCs	0.638	0.294	0.662	0.9178	2.7239
BiOCl-NCs-OV	0.734	0.465	0.791	0.7581	2.4761

Figure S8. The relative band intensity of I2/I1 and I3/I1.

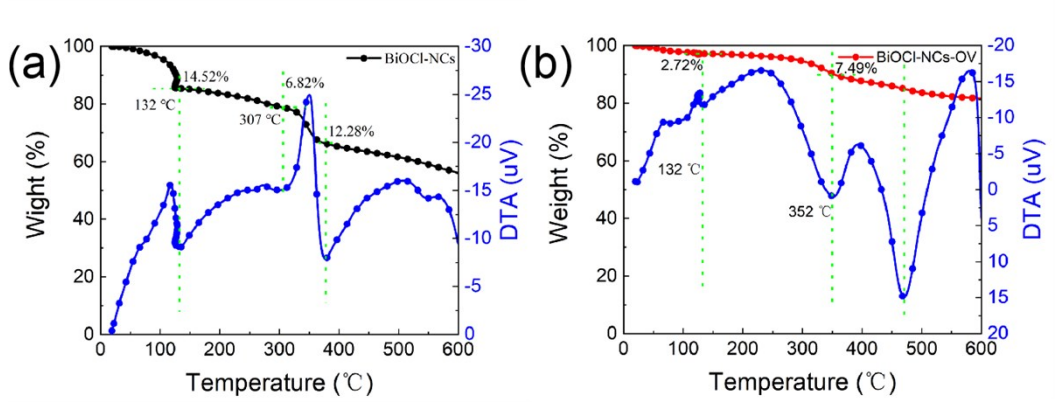

Figure S9. Thermogravimetric analysis of (a) BiOCl-NCs and (b) BiOCl-NCs-OV.

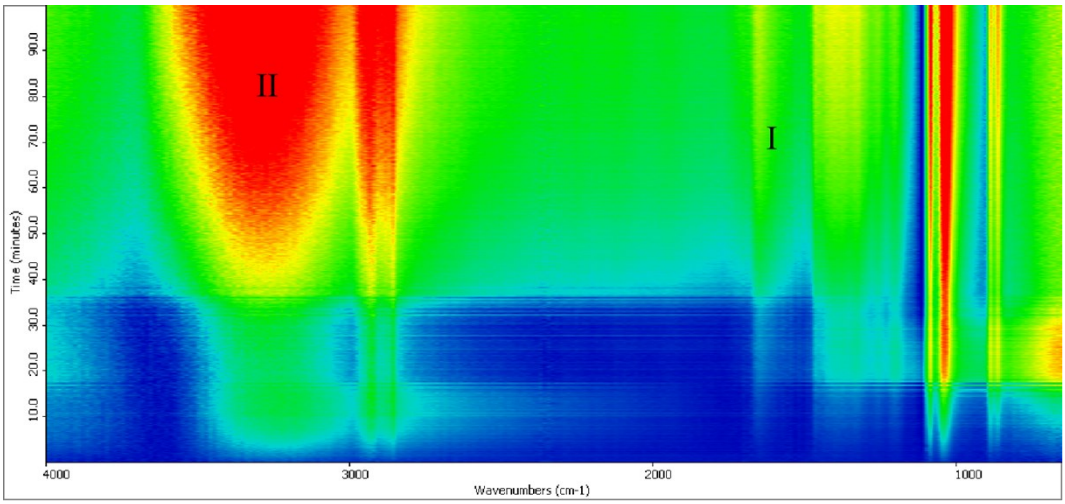

Figure S10. In situ FT-IR spectra of the photoactivation process on BiOCl-NCs-OV.

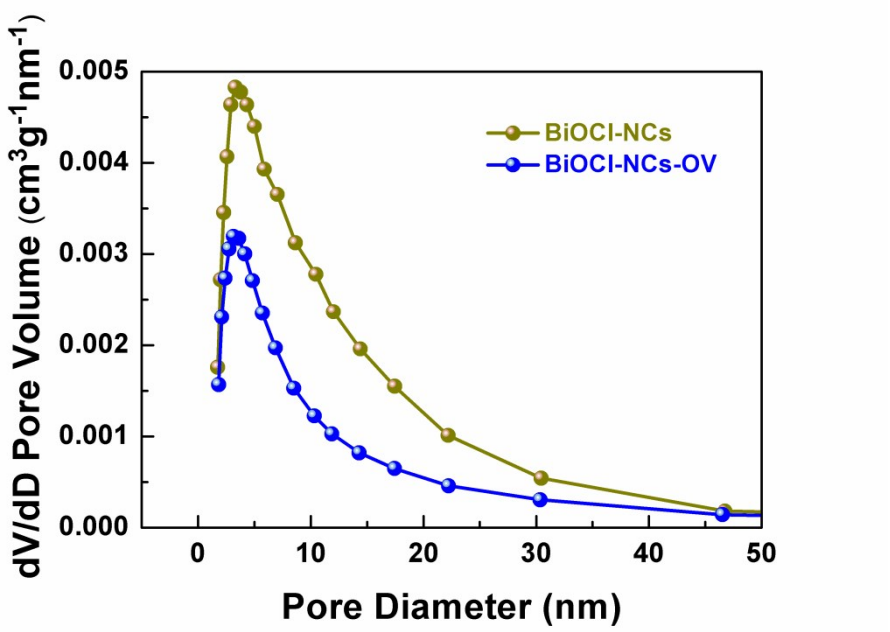

Figure S11. The pore size distribution curve determined from BJH method of BiOCl-NCs and BiOCl-NCs-OV.

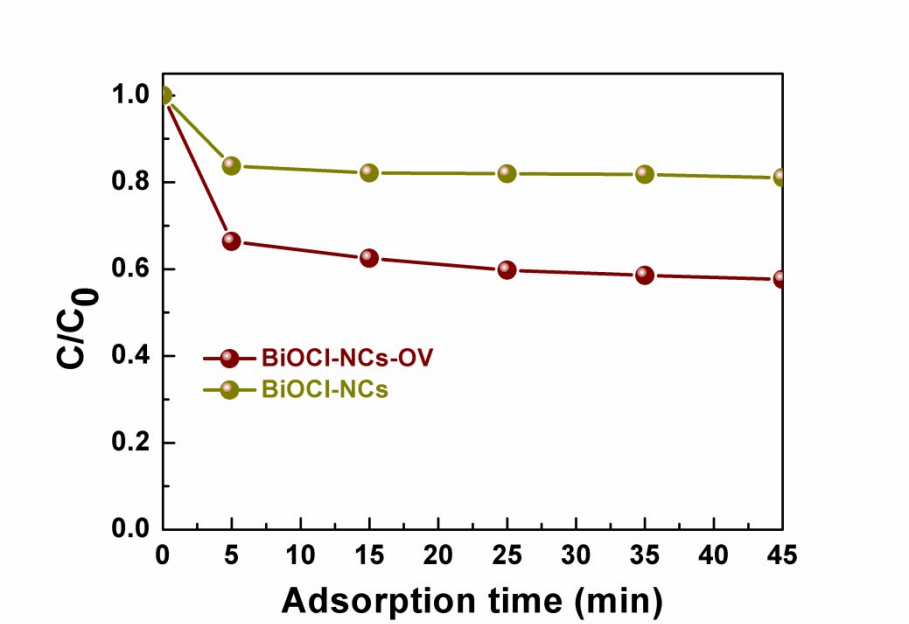

Figure S12. The adsorption kinetic of BiOCl-NCs and BiOCl-NCs-OV for RhB in dark condition under vigorous stirring.

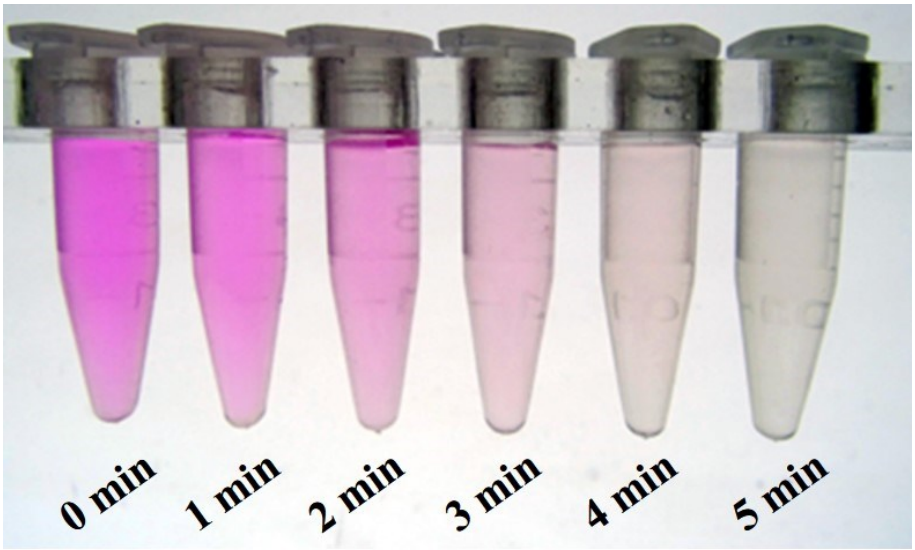

Figure S13. Color change of residual RhB solution during degradation with BiOCl-NCs-OV catalyst.

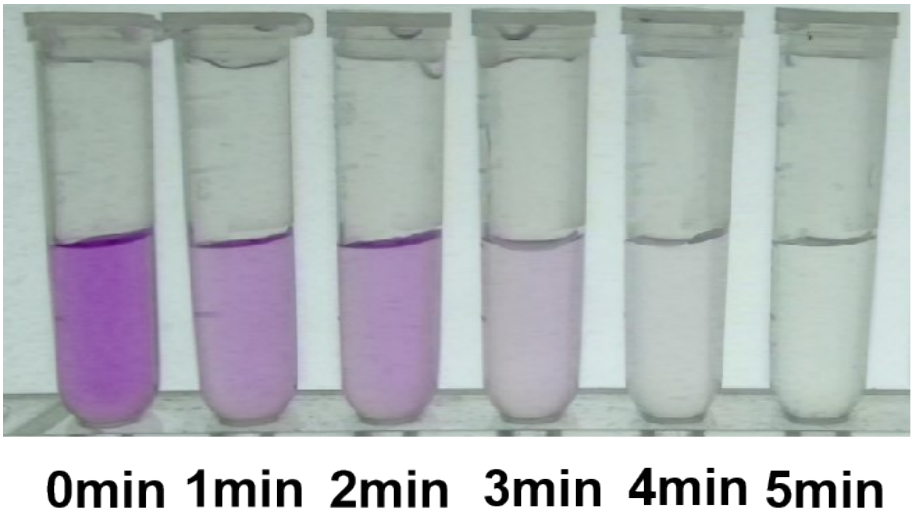

Figure S14. Color change of residual Cr(Ⅵ) solution during degradation with BiOCl-NCs-OV catalyst.

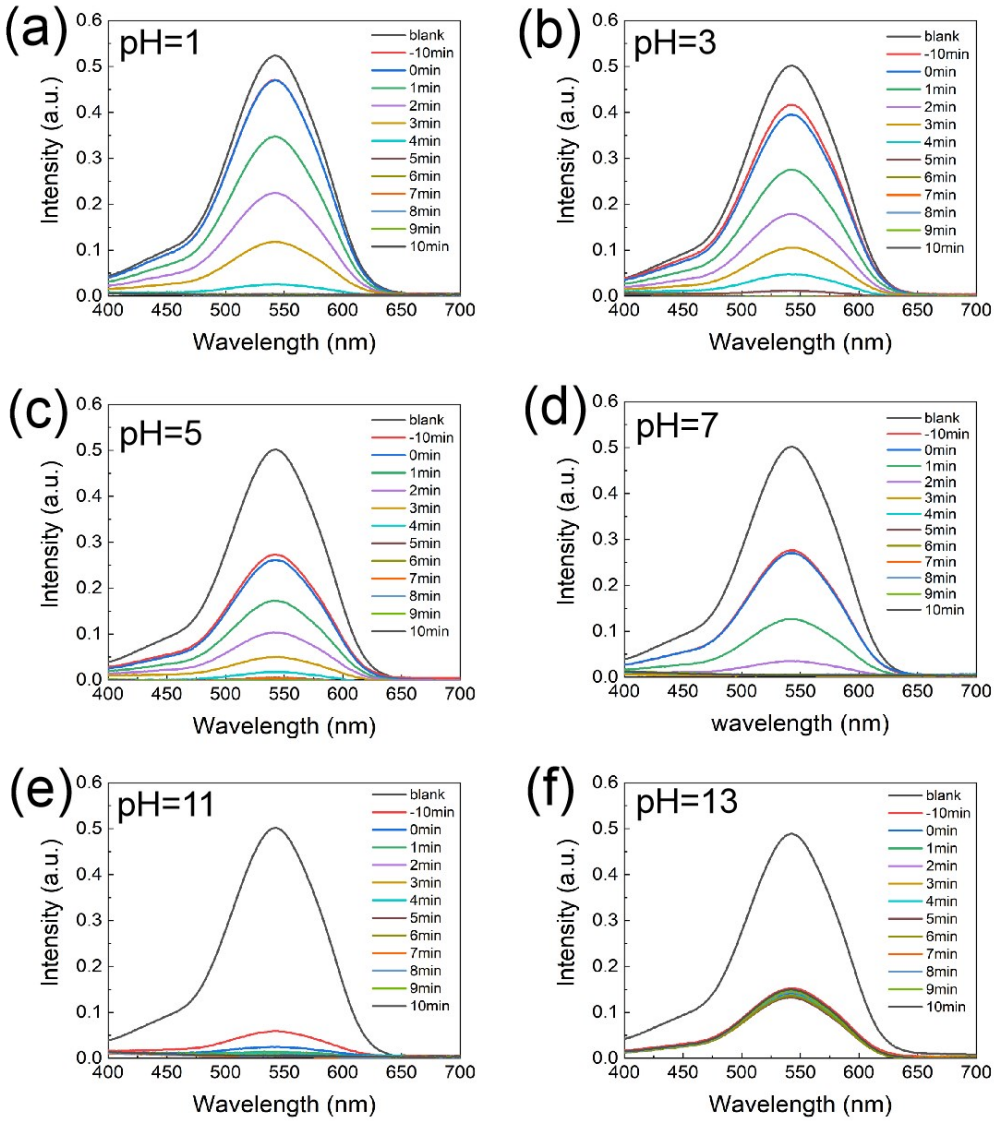

Figure S15. UV-Vis spectral evolution of Cr(Ⅵ) solution in the presence of BiOCl-NCs-OV under different pH condition.

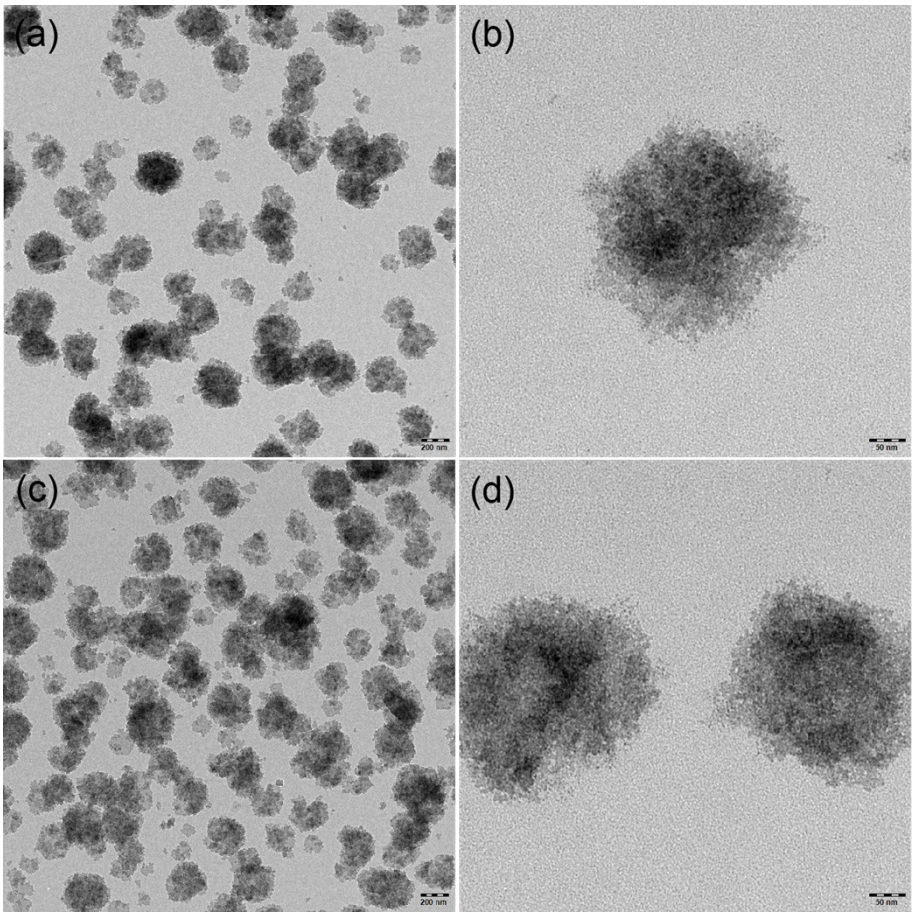

Figure S16. (a, c) Low-magnification and (b, d) high-magnification TEM images of BiOCl-NCs-OV after the stability test for RhB and Cr(Ⅵ) degradation, respectively.

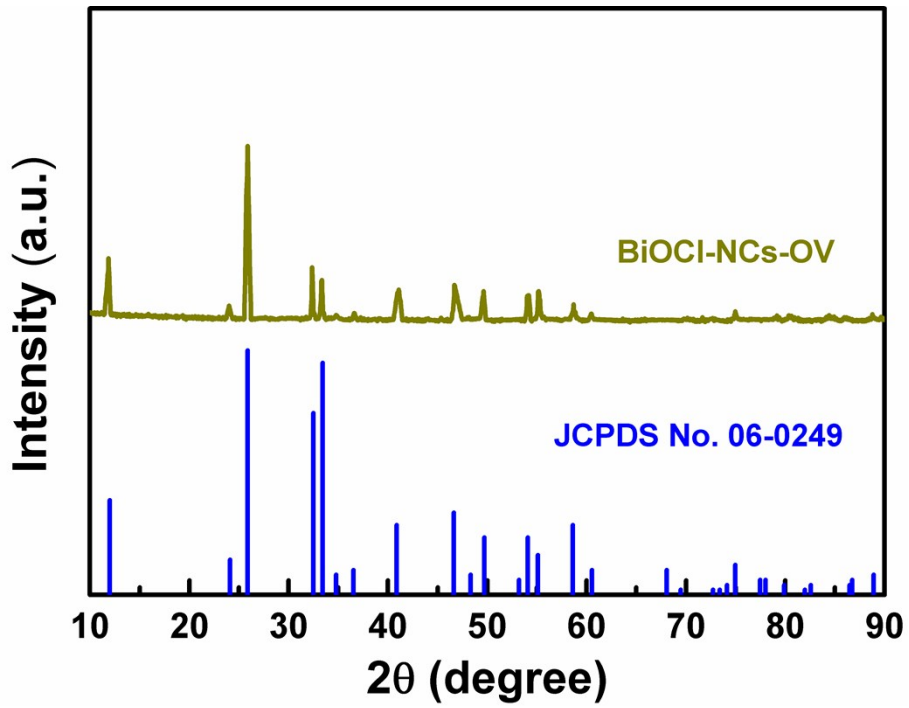

Figure S17. XRD pattern after the stability test for RhB degradation.

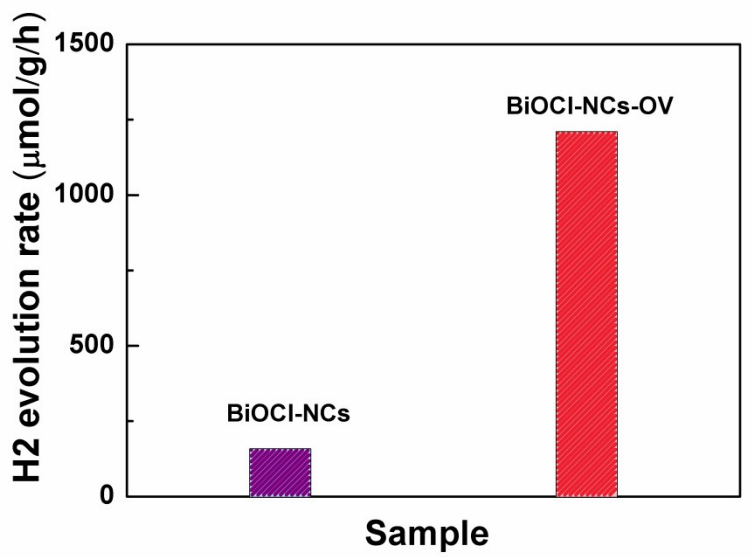

Figure S18. Photocatalytic H_2 production activity of of BiOCl-NCs-OV and BiOCl-NCs.

Table S1. Comparisons of RhB/Cr degradation performance for various photocatalysts.

Catalysts	Contaminants	Activity (degradation Time)	reference
BiOCl-NCs-OV	RhB/Cr	**4min/3min**	This work
TiO_2/ZrO_2	RhB	240min	1
Bi_2WO_6	RhB/Cr	45min/30min	2
$LaFeO_3/Ag_2CO_3$	RhB	45min	3
Tb_xO_y/TiO_2 nanosheets	Cr	30min	4
$CdS/CuInS_2$ nanoplates	Cr	60min	5
$FeWO_4/g\text{-}C_3N_4$	RhB	90min	6
Bi_2WO_6 microspheres	RhB	30min	7

rGO/Bi_2S_3-BiOBr	Cr	120min	8

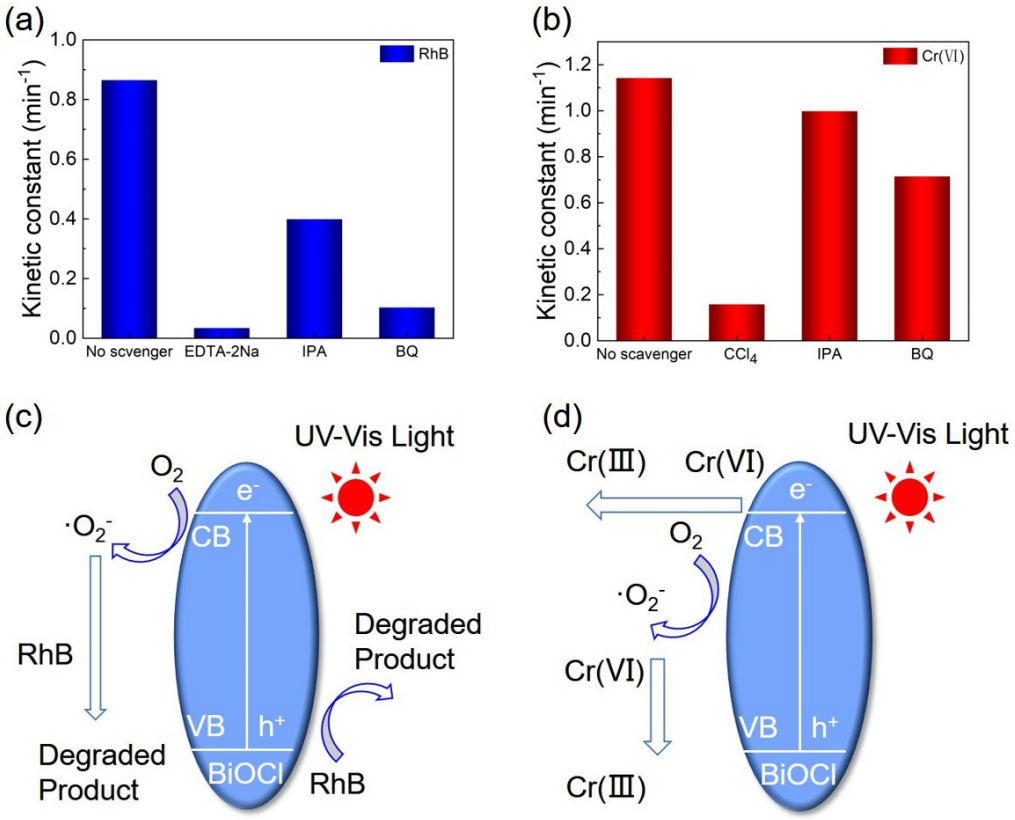

Figure S19. (a) Photocatalytic degradation of RhB and (b) reduction of Cr(Ⅵ) over BiOCl-NCs-OV in the presence of active species trapping scavengers. (c) The proposed RhB degration and (d) Cr(Ⅵ) reduction processes of the BiOCl-NCs under UV-vis light.

Notes for S19. When BiOCl-NCs is exposed to light, the Bi-OH bonds on its surface will break, and water and surface oxygen defects will rapidly form. The electrons in the VB of BiOCl-NCs-OV are first excited to the CB or OV levels, and the holes are formed in the VB. Water adsorbed on the surface of BiOCl-NCs-OV is oxidized by the holes to form a peroxide adsorbed on the surface. Subsequently, the photogenerated electrons and holes respectively migrate to two opposite direction along [001] zone axis of BiOCl-NCs with the assistance of the internal electric field induced by layered crystal structures. Furthermore, the photoinduced charge carriers in BiOCl nanoclusters facilely reach their top and bottom planes to participate in the surface reactions due to

the short transfer distance. Finally, the photoexcited electrons react with surface bonded O_2 to produce $\cdot O_2^-$ radicals that degrade RhB molecules and Cr(Ⅵ) ions. Meanwhile, the absorbed contaminants such as RhB and Cr(Ⅵ) can also be decomposed by the holes enriched on another surface. In brief, the degradation of RhB in the present study is substantial a photooxidation process, while the reduction of Cr(Ⅵ) is a photoreduction process. The $\cdot O_2^-$ radicals can be used not only to oxidize organic pollutants such as rhodamine B, but also to reduce hexavalent chromium ions.

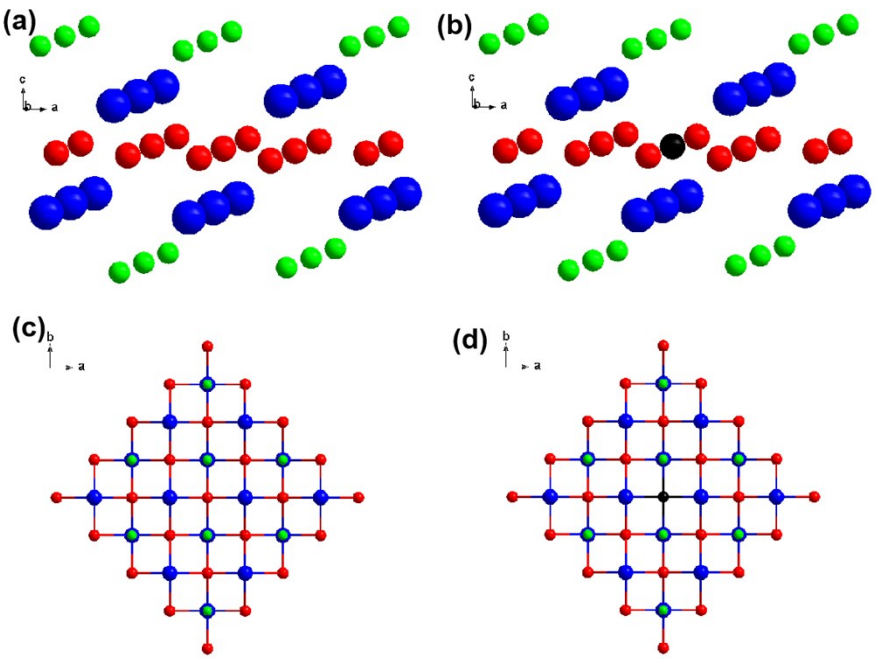

Figure S20. Simulated crystal structure of (a) BiOCl and (b) BiOCl with oxygen vacancies. Top view of (001) facet of (c) BiOCl and (d) BiOCl with oxygen vacancies. Color denotation: blue (Bi), green (Cl), red (O), and black (O_v).

Reference:

[1] Jiangyang Tian, Qian Shao, Junkai Zhao, Duo Pan, Mengyao Dong, Chengxinzhuo Jia, Tao Ding, Tingting Wu, Zhanhu Guo, Microwave solvothermal carboxymethyl chitosan templated synthesis of TiO_2/ZrO_2 composites toward enhanced photocatalytic degradation of Rhodamine B, *Journal of Colloid and Interface Science,* 2019, 541, 18-29.

[2] Tianye Wang, Shuxia Liu, Wei Mao, Yichen Bai, Ken Chiang, Kalpit Shah, JorgePaz Ferreiro, Novel Bi_2WO_6 loaded N-biochar composites with enhanced photocatalytic degradation of rhodamine B and Cr(VI), *Journal of Hazardous Materials*, 2020, 289, 121827.

[3] Bilal M. Pirzada, Pushpendra, Ravi K. Kunchala, Boddu S. Naidu, Synthesis of $LaFeO_3/Ag_2CO_3$ Nanocomposites for Photocatalytic Degradation of Rhodamine B and p-Chlorophenol under Natural Sunlight, *ACS Omega,* 2019, 4, 2618-2629.

[4] Dingze Lu, Minchen Yang, Pengfei Fang, Chunhe Li, Lulu Jiang, Enhanced photocatalytic degradation of aqueous phenol and Cr(VI) over visible-light-driven Tb_xO_y loaded TiO_2-oriented nanosheets, *Applied Surface Science*, 2017, 399, 167-184.

[5] Fang Deng, Xiaoying Lu, Yingbo Luo, Jie Wang, Wenjie Che, Ruijie Yang, Xubiao Luo, Shenglian Luo, Dionysios D. Dionysiou, Novel visible-light-driven direct Z-scheme $CdS/CuInS_2$ nanoplates for excellent photocatalytic degradation performance and highly-efficient Cr(VI) reduction, *Chemical Engineering Journal*, 2019, 361, 1451-1461.

[6] Ramakrishna Dadigala, RajKumar Bandi, Bhagavanth Reddy Gangapuram, Veerabhadram Guttena, Construction of in situ self-assembled $FeWO_4/g\text{-}C_3N_4$ nanosheet heterostructured Z-scheme photocatalysts for enhanced photocatalytic degradation of rhodamine B and tetracycline, *Nanoscale Adv*, 2019, 1, 322-333.

[7] Xianghui Zhang, Mingming Zhang, Kaixuan Cao, Hydrothermal synthesis of Sm-doped Bi_2WO_6 flower-like microspheres for photocatalytic degradation of rhodamine B, *CrystEngComm*, 2019, 21, 6208-6218.

[8] Hui Li, Fang Deng, Yang Zheng, Li Hua, Chunhua Qu, Xubiao Luo, Visible-light-driven Z-scheme rGO/Bi_2S_3-BiOBr heterojunctions with tunable exposed BiOBr (102) facets for efficient synchronous photocatalytic degradation of 2-nitrophenol and Cr(vi) reduction, *Environ. Sci.: Nano*, 2019,6, 3670-3683.